Research Square

Preprints are preliminary reports that have not undergone peer review.
They should not be considered conclusive, used to inform clinical practice,
or referenced by the media as validated information.

Combined evaluation of stress hyperglycemia ratio and glycemic variability stratified by glucose metabolic status in critically ill cerebrovascular disease: a retrospective study with machine learning

Zhantao Cao
China Academy of Chinese Medical Sciences
Siyu Liu
China Academy of Chinese Medical Sciences
Yue Wei
China Academy of Chinese Medical Sciences
Dongxin Liu
China Academy of Chinese Medical Sciences
Yao Li
China Academy of Chinese Medical Sciences
Guoju Dong
136913935890163.com

China Academy of Chinese Medical Sciences

Research Article

Keywords: Cerebrovascular disease, Stress hyperglycemia ratio, Glycemic variability, MIMIC-IV database, Machine learning

Posted Date: May 12th, 2026

DOI: https://doi.org/10.21203/rs.3.rs-9458260/v1

License: This work is licensed under a Creative Commons Attribution 4.0 International License.
Read Full License

Additional Declarations: No competing interests reported.

Abstract

Background

The stress hyperglycemia ratio (SHR) indicates how much glucose rises acutely relative to baseline, whereas glycemic variability (GV) captures short-term swings in glucose levels. However, the added value of their combined assessment, as well as the modulatory impact of different glucose metabolic states on their prognostic impact, remains unclear.

Methods

We performed a retrospective cohort analysis based on data obtained from the MIMIC-IV database. Adult critically ill patients with cerebrovascular disease were included and classified by glucose metabolic status. We calculated the SHR and GV, then grouped them by quantiles and by combined strata. Associations were evaluated using Kaplan–Meier survival analysis, multivariable Cox regression models, restricted cubic splines (RCS), subgroup analyses, and landmark analyses. Discriminative ability was compared through receiver operating characteristic curves. In addition, several machine learning models were built, key variables were selected using Boruta, and Shapley additive explanations were applied to explain the model with the highest performance.

Result

In total, 4,441 patients were enrolled, and the mortality rate within 28 days was 12.2%. Multivariable Cox analysis showed that higher SHR was associated with an increased risk of 28-day mortality, with the strongest association observed in the NGR group (HR 2.07, 95% CI 1.27–3.38, P = 0.004). Higher GV was also associated with increased mortality risk, mainly in the NGR group (HR 2.48, 95% CI 1.62–3.80, P < 0.001). After combined stratification, the risk gradient became clearer. Patients with both elevated SHR and increased GV showed the greatest risk (HR 1.84, 95% CI 1.43–2.37, P < 0.001). This association was even stronger in the NGR group (HR 2.87, 95% CI 1.79–4.61, P < 0.001). Landmark analysis indicated that there was no significant difference between the groups during the first 2 days following ICU admission (P = 0.130), while a significant difference emerged after 2 days (P = 0.008). In ROC analysis, the combined metric achieved a maximum AUC of 0.686 in the NGR group, whereas the best-performing machine learning model reached an AUC of 0.851.

Conclusion

Among critically ill patients with cerebrovascular disease, evaluating SHR together with GV enhances risk stratification for 28-day mortality.

1. Introduction

Cerebrovascular disease continues to be a major contributor to death and long-term disability around the world. Recent findings from the Global Burden of Disease study indicate that mortality and disability related to stroke were still substantial in 2021 (1, 2). Once patients with cerebrovascular disease progress to a critical condition, clinical outcomes are often worse. Studies indicate that patients with acute ischemic stroke admitted to a stroke unit or ICU have an in-hospital mortality of approximately 6% to 8% (3). In patients with spontaneous intracerebral hemorrhage, studies using intensive care databases have reported high in-hospital and ICU mortality, with several metabolic markers strongly linked to death (4). In addition, long-term follow-up studies in type 2 diabetes mellitus (T2DM) have shown a higher risk of adverse cardiovascular outcomes, while different diagnostic criteria for prediabetes (PreDM) are linked to different levels of risk. These findings indicate marked clinical heterogeneity across glucose metabolic phenotypes (5, 6).

Against this background of heterogeneous glucose metabolic states, transient elevations in blood glucose are common during acute cerebrovascular events. This phenomenon is known as stress hyperglycemia (7). The primary mechanism is the activation of the sympathetic nervous system and the hypothalamic–pituitary–adrenal axis in response to acute stress. As a result, hepatic glucose output rises and insulin resistance develops, causing short-term hyperglycemia (8, 9). The stress hyperglycemia ratio (SHR) is applied to quantify the relative extent of hyperglycemia triggered by stress. It integrates admission average glucose (AG) with the background of chronic glycemia assessed by HbA1c. Recent studies have demonstrated that higher SHR levels are associated with increased all-cause mortality in patients with acute myocardial infarction(AMI) complicated by diabetes and in those with new-onset atrial fibrillation(AF) (10, 11). Glycemic variability (GV) refers to the extent of glucose fluctuations over a specified period of time. It is commonly quantified using measures such as the standard deviation and the CV (12). Repeated swings between glucose peaks and nadirs are more likely to trigger oxidative stress and inflammatory cascades. These mechanisms may damage endothelial function and promote pathological states, including atherosclerosis (13). Several studies have linked higher GV to adverse outcomes across different diseases, including sepsis and coronary artery disease (14, 15).

Different glucose metabolic states also influence the interpretation of chronic glycemic background and acute glucose elevation. The same admission glucose level may therefore carry different relative risk signals across diabetic states. Earlier stratified analyses in critically ill patients with spontaneous intracerebral hemorrhage have indicated that the prognostic value of SHR varies between individuals with diabetes and those without diabetes. This highlights the need for stratified evaluation by glucose metabolic status (16). Similarly, GV is not limited to patients with diabetes. Continuous glucose monitoring studies have shown that non-diabetic patients in acute stroke cohorts may also experience marked fluctuations and occult hypoglycemia. This supports the inclusion of glucose variability as a risk phenotype in patients with normal glucose regulation (NGR) and PreDM (17).

However, the prognostic roles of SHR, GV, and their combined measures in critically ill patients with cerebrovascular disease across different glucose metabolic phenotypes are still uncertain. Therefore, we set out to systematically assess how well SHR, GV, and their combination predict all-cause mortality in critically ill cerebrovascular disease patients, stratified by glucose metabolic status.

2. Methods

2.1. Data source

This study analyzed patient records from the MIMIC-IV database (version 3.1)(18). The database offers rich patient-level information, including demographics, diagnostic groups, vital signs, laboratory tests, medication records, and discharge outcomes. One investigator, Zhantao Cao, completed the required CITI ethics training and received approved access to the MIMIC-IV dataset (certification number: 14336451). All data extraction and processing were carried out in strict accordance with the database guidelines and relevant ethical requirements. All data extraction and processing were carried out in strict accordance with the database guidelines and relevant ethical requirements. Clinical trial number: not applicable.

2.2 Participants

Critically ill cerebrovascular disease was identified using the ICD-9) and ICD-10 codes (19, 20) (Table S1). Only patients with cerebrovascular disease who were admitted to the ICU for their first ICU stay were included. Patients were excluded based on predefined criteria, including age under 18 years, an ICU stay shorter than 24 hours, absence of outcome data or key prognostic variables, fewer than three glucose measurements during the ICU stay, or unavailable HbA1c values. The study flowchart is shown in Fig. 1.

2.3 Data collection

Data were obtained from the MIMIC-IV database through SQL queries using pgAdmin version 4. All variables were collected from clinical records documented within the first 24 hours after ICU admission. In detail, data were gathered across seven distinct categories: demographic characteristics, vital signs, baseline comorbidities, laboratory parameters, medication exposure, therapeutic interventions, and illness severity scores. The primary endpoint of this study was all-cause mortality within 28 days. A detailed list of all variables is presented in Table S2.

SHR was computed according to the following formula: SHR = [ABG (mg/dL)/(28.7 × HbA1c (%) − 46.7)] (21). As the database did not contain information on meal timing, all sequential glucose measurements recorded during the ICU stay were included in the analysis. This approach better reflects real-world glucose monitoring in the ICU and is consistent with previous critical care studies (22–24). GV was primarily evaluated using the coefficient of variation(CV). CV was calculated as the SD divided by the mean glucose level, multiplied by 100% (25). Both SD and mean values were derived from all glucose measurements recorded during ICU monitoring. CV is easy to interpret and allows comparison across patients with different baseline glucose levels.

Patients were classified into three groups based on HbA1c levels and prior history of diabetes: normal NGR, defined as HbA1c less than 5.7% with no history of diabetes; PreDM, defined as HbA1c from 5.7% to less than 6.5% with no history of diabetes; and DM, defined as a known history of diabetes or HbA1c of 6.5% or higher (26).

SHR and GV were further stratified into tertiles. The highest tertile was defined as high, and the remaining tertiles were defined as low. These categories were combined to form four groups: low SHR plus low GV, low SHR plus high GV, high SHR plus low GV, and high SHR plus high GV. These groups were used for subsequent survival analyses and model comparisons. To handle missing data and limit potential bias, variables with over 20% missing values were removed. For variables with less than 20% missing data, multiple imputation was conducted using the mice package in R.

2.4 Statistical analysis

Normality of continuous variables was tested with the Kolmogorov–Smirnov test. These variables are reported as mean ± SD or as median with IQR, as appropriate. Categorical variables are shown as counts and percentages. Group comparisons used the t test or one-way analysis of variance for normally distributed data, and the Kruskal–Wallis test for non-normal data.

Kaplan–Meier(KM) survival curves were used to display cumulative all-cause mortality across groups. We then ran univariable Cox regression to identify variables that might be associated with all-cause mortality (Table S3). Multicollinearity among candidate covariates was evaluated using the variance inflation factor (VIF). A VIF above 5 was taken as evidence of substantial multicollinearity, and variables meeting this criterion were removed from the multivariable models. (Table S4). Restricted cubic splines were applied to explore possible nonlinear relationships between SHR, GV, and all-cause mortality.

Stepwise Cox proportional hazards models were subsequently built to control for potential confounders. Model 1 included no covariate adjustment. Model 2 adjusted for age, sex, and race. Model 3 included additional adjustments, based on univariable Cox results and clinical relevance, for Acute Physiology Score III (APS-III), Glasgow Coma Scale (GCS), heart rate (HR), respiratory rate (RR), oxygen saturation (SpO_2), temperature, creatinine (Cr), white blood cell count (WBC), platelet count, AF, heart failure (HF), hypertension, MI, chronic obstructive pulmonary disease (COPD), and mechanical ventilation. The proportional hazards assumption was evaluated using Schoenfeld residuals.

Landmark analysis was conducted to evaluate time-related changes in the association between exposures and the risk of mortality. To compare how well different indicators predicted 28-day all-cause mortality, we constructed receiver operating characteristic curves and calculated the area under the curve. The indicators included SHR, GV, their combined measure, and commonly used severity scores. Discrimination was assessed by the AUC.

To assess the consistency of the findings across populations, subgroup analyses were conducted according to age, sex, major comorbidities, and treatment strategies. Finally, multiple sensitivity analyses were performed by repeating the main models to evaluate the robustness of the results.

2.5 Construction and assessment of the prognostic models

To further improve model performance and reduce feature redundancy, we applied the Boruta algorithm for feature selection. Boruta generates randomly permuted shadow features and compares their importance with that of the original variables, thereby identifying features that make a meaningful contribution to the outcome. We subsequently chose the 15 most important variables from the Boruta confirmed set for further model construction and validation.

The dataset was randomly divided into a training set comprising 70% of the data and a testing set comprising the remaining 30%. Hyperparameter tuning was performed for six machine learning algorithms, including RF, k-nearest neighbors (KNN), extreme gradient boosting (XGBoost), decision tree (DT), support vector machine (SVM), and light gradient boosting machine (LGBM). Model discrimination was evaluated in the testing set using ROC curves and AUC. To further evaluate clinical usefulness, we performed decision curve analysis. We also plotted calibration curves to assess agreement between predicted risks and observed outcomes. Finally, SHAP values were computed for each variable to quantify the direction and strength of its contribution to outcome prediction. Features were then ranked according to SHAP importance, and visualizations were used to illustrate how different feature values influenced the predicted risk. All analyses were carried out using R software version 4.4.2 and DecisionLnnc 1.0. Statistical significance was defined as a two-sided p value below 0.05.

3. Results

3.1. Baseline characteristics

The final analysis included 4,441 patients in total. Among them, 3,898 patients (87.8%) survived and 543 patients (12.2%) died within 28 days after ICU admission. The overall median age was 71 years, and 2,381 patients (54%) were male. Regarding glucose metabolic status, NGR, PreDM, and DM accounted for 37%, 25%, and 38% of the cohort, respectively.

Compared with 28-day survivors, non-survivors were older and differed in racial distribution. In early vital signs after ICU admission, non-survivors had HR and RR, and lower mean noninvasive blood pressure (NBPM). In laboratory findings, non-survivors had lower hemoglobin (Hb) and red blood cell count (RBC), but higher WBC, potassium, Cr, blood urea nitrogen, and prothrombin time (PT). In addition, non-survivors had higher SHR, higher glucose levels, and greater GV. In terms of comorbidities and treatments, AF, HF, and MI were more common among non-survivors. Non-survivors were more likely to receive vasoactive agents and mechanical ventilation(Table 1).

Table 1
Baseline characteristics of the overall cohort by 28-day survival status.

Characteristic	Overall (n = 4,441)	Survivor_28d (n = 3,898)	NonSurvivor_28d (n = 543)	*p*-value
Age (year)	71 (60–81)	70 (59–80)	74 (64–84)	< 0.001
Gender, n (%)				0.3
Female	2,060 (46%)	1.796 (46%)	264 (49%)	
Male	2,381 (54%)	2,102 (54%)	279 (51%)	
Race, n (%)				< 0.001
WHITE	2,515 (57%)	2,273 (58%)	242 (45%)	
BLACK	504 (11%)	452 (12%)	52 (9.6%)	
OTHERS	1,422 (32%)	1,173 (30%)	249 (46%)	
HR (bpm)	82 (71–96)	82 (71–96)	86 (71–100)	0.001
RR (bpm)	18.0 (16.0–22.0)	18.0 (16.0–22.0)	19.0 (16.0–23.0)	0.002
Temperature (°C)	98.20 (97.80–98.80)	98.30 (97.80–98.80)	98.20 (97.70–98.80)	0.4
SpO2 (%)	98.00 (95.00-100.00)	98.00 (95.00-100.00)	98.00 (96.00-100.00)	< 0.001
NBPM (mmHg)	91 (80–103)	92 (80–103)	88 (76–102)	0.002
Hb (g/dL)	12.10 (10.50–13.50)	12.20 (10.60–13.60)	11.50 (9.70–12.90)	< 0.001
Plt (10^9/L)	209 (164–263)	209 (165–263)	201 (148–266)	0.014
RBC (10^9/L)	4.04 (3.54–4.50)	4.07 (3.58–4.52)	3.81 (3.24–4.35)	< 0.001
WBC (10^9/L)	10.1 (7.8–13.3)	9.9 (7.7–13.0)	11.5 (8.5–15.9)	< 0.001
Potassium (mmol/L)	4.00 (3.70–4.40)	4.00 (3.70–4.40)	4.10 (3.70–4.60)	< 0.001
Sodium (mmol/L)	139.0 (137.0-141.0)	139.0 (137.0-141.0)	139.0 (136.0-142.0)	0.4
Cr (mg/dL)	0.90 (0.70–1.30)	0.90 (0.70–1.20)	1.00 (0.80–1.50)	< 0.001
BUN (mg/dL)	17 (13–25)	17 (12–25)	21 (15–34)	< 0.001

Characteristic	Overall (n = 4,441)	Survivor_28d (n = 3,898)	NonSurvivor_28d (n = 543)	*p*-value
PT (S)	12.90 (11.80–14.30)	12.90 (11.80–14.10)	13.70 (12.30–15.70)	< 0.001
HbA1c (%)	5.80 (5.40–6.50)	5.80 (5.40–6.50)	5.90 (5.40–6.70)	0.2
SHR	1.03 (0.87–1.25)	1.02 (0.87–1.23)	1.14 (0.92–1.43)	< 0.001
Glu (mg/dL)	126 (104–162)	125 (103–158)	140 (111–190)	< 0.001
GV(%)	18 (12–27)	18 (12–26)	22 (14–32)	< 0.001
AF, n (%)	1,506 (34%)	1,257 (32%)	249 (46%)	< 0.001
Diabetes, n (%)	1,579 (36%)	1,373 (35%)	206 (38%)	0.2
Hypertension, n (%)	2,456 (55%)	2,173 (56%)	283 (52%)	0.12
HF, n (%)	1,097 (25%)	928 (24%)	169 (31%)	< 0.001
MI, n (%)	401 (9.0%)	322 (8.3%)	79 (15%)	< 0.001
COPD, n (%)	431 (9.7%)	378 (9.7%)	53 (9.8%)	> 0.9
VP, n (%)	1,482 (33%)	1,167 (30%)	315 (58%)	< 0.001
HA, n (%)	263 (5.9%)	259 (6.6%)	4 (0.7%)	< 0.001
IA, n (%)	3,495 (79%)	3,036 (78%)	459 (85%)	< 0.001
Ventilation, n (%)	3,006 (68%)	2,562 (66%)	444 (82%)	< 0.001
APS - III	37 (28–48)	36 (27–47)	45 (34–59)	< 0.001
SAPS - II	32 (25–40)	31 (25–39)	38 (32–46)	< 0.001
GCS	14.00 (12.00–15.00)	14.00 (12.00–15.00)	15.00 (11.00–15.00)	0.053
SOFA	3 (2–5)	3 (2–5)	4 (2–7)	< 0.001
Glucose metabolism state				0.012
NGR	1,632 (37%)	1,459 (37%)	173 (32%)	
Pr-DM	1,110 (25%)	977 (25%)	133 (24%)	
DM	1,699 (38%)	1,462 (38%)	237 (44%)	

HR Heart Rate; RR Respiratory Rate; SpO2 O2 saturation pulseoxymetry; NBPM Non Invasive Blood Pressure mean; Hb hemoglobin; Plt platelet; RBC red blood cell; WBC white blood cell; Cr creatinine;

Characteristic	Overall (n = 4,441)	Survivor_28d (n = 3,898)	NonSurvivor_28d (n = 543)	*p*-value

BUN blood urea nitrogen; PT prothrombin time; HbA1c glycated hemoglobin; SHR stress hyperglycemia ratio; Glu glucose; GV glycemic variability; AF atrial fibrillation; HF heart failure; MI myocardial infarction; COPD chronic obstructive pulmonary disease; VP Vasopressor; HA Hypoglycemic Agents; IA Insulin Therapy; APS-III acute physiology score III; SAPS-II simplified acute physiology score II; GCS Glasgow coma scale; SOFA sequential organ failure assessment; NGR normal glucose regulation; Pr-DM prediabetes mellitus; DM diabetes mellitus.

3.2. The association between SHR and mortality

KM survival curves demonstrated a stepwise reduction in 28-day survival as SHR tertiles increased across different glucose metabolic states (Fig. 2A, D, G). In the fully adjusted Cox regression model (Model 3), patients in the highest SHR tertile (T3) showed a greater risk of 28-day mortality compared with those in the lowest tertile (T1) in the overall cohort (HR 1.41, 95% CI 1.14–1.75, P = 0.002). After stratification by glucose metabolic status, this association was most pronounced in the NGR group (T3 vs T1: HR 2.07, 95% CI 1.27–3.38, P = 0.004). In the PreDM and DM groups, the increased risk associated with T3 was not statistically significant after full adjustment (Table S5).

Restricted cubic spline analysis revealed a nonlinear relationship between SHR and mortality risk in the NGR group. No clear nonlinear pattern was observed in the PreDM or DM groups (Fig. 3A). Subgroup analyses (Fig. 6A) showed that the direction of the association between SHR, modeled per 1 standard deviation increase, and 28-day mortality was generally consistent across strata defined by age, sex, and major comorbidities or treatments. No significant interaction effects were detected.

3.3. The association between GV and mortality

KM curves showed that higher GV tertiles were associated with lower 28-day survival in the NGR and PreDM groups (Fig. 2B, 2E, 2H). In multivariable Cox regression, patients in the highest GV tertile had a greater risk of 28-day all-cause mortality compared with the lowest tertile in the overall cohort (HR 1.32, 95% CI 1.04–1.66, P = 0.020). Stratified analyses showed that this association was mainly observed in the NGR group (T3 vs T1: adjusted HR 2.48, 95% CI 1.62–3.80, P < 0.001; P for trend = 0.001). No significant risk increase was observed in the PreDM or DM groups (Table S5).

Restricted cubic spline analysis was further used to examine the dose–response relationship between GV and mortality. A significant overall association was identified only in the NGR group, while no significant relationship was observed in the PreDM or DM groups (Fig. 3B). Subgroup analyses based on a 1 standard deviation increase in GV showed no significant overall effect. However, an age-related interaction was identified. GV was linked to a higher risk of mortality in patients younger than 65 years, whereas this association was weaker in patients aged 65 years or older (P for interaction = 0.036; Fig. 6B).

3.4. The association of combined SHR and GV with mortality

The 28-day survival across the combined SHR and GV groups is shown in Fig. 2C, F, and I. Overall, survival curves progressively separated as the combined SHR and GV risk increased. The group with both high SHR and high GV showed the lowest survival. The combined groups were defined as follows: Group 1 with low SHR and low GV, Group 2 with low SHR and high GV, Group 3 with high SHR and low GV, and Group 4 with high SHR and high GV. The corresponding cutoffs were an SHR of 1.17 and a GV of 23.40.

In multivariable Cox regression analysis (Model 3), using Group 1 as the reference, all other groups showed higher mortality risk in the overall cohort. Group 4 had the highest risk (HR 1.84, 95% CI 1.43–2.37, P < 0.001; P for trend < 0.001). Stratified analyses showed that the combined effect was most evident in the NGR group. Group 4 had the highest mortality risk (HR 2.87, 95% CI 1.79–4.61, P < 0.001), and Group 3 also showed a significant increase in risk (HR 1.82, 95% CI 1.24–2.68, P = 0.002). Group 2 showed only a borderline association after full adjustment (P = 0.073). In the PreDM group, increased risk was mainly observed in Group 2 (HR 2.15, 95% CI 1.34–3.46, P = 0.001) and Group 3 (HR 1.70, 95% CI 1.07–2.72, P = 0.026). Group 4 did not reach statistical significance in Model 3 (HR 1.50, 95% CI 0.82–2.74, P = 0.192; P for trend = 0.044). In contrast, no stable risk increase was observed for the combined metric in the DM group under Model 3 (Table 2).

Table 2
The association of the combination of SHR and GV with all-cause mortality

Variables	Model 1		Model2		Model3	
	HR (95%CI)	*P*	HR (95%CI)	*P*	HR (95%CI)	*P*
Overall						
Group 1	1.00 (Reference)		1.00 (Reference)		1.00 (Reference)	
Group 2	1.95 (1.54–2.47)	< 0.001	1.89 (1.49–2.39)	< 0.001	1.54 (1.20–1.96)	< 0.001
Group 3	1.97 (1.56–2.49)	< 0.001	1.89 (1.49–2.39)	< 0.001	1.47 (1.16–1.87)	0.002
Group 4	2.79 (2.22–3.50)	< 0.001	2.74 (2.18–3.44)	< 0.001	1.84 (1.43–2.37)	< 0.001
P for trend		< 0.001		< 0.001		< 0.001
DM						
Group 1	1.00 (Reference)		1.00 (Reference)		1.00 (Reference)	
Group 2	1.27 (0.90–1.79)	0.176	1.28 (0.90–1.81)	0.165	1.17 (0.81–1.68)	0.395
Group 3	1.26 (0.80–1.98)	0.313	1.19 (0.76–1.87)	0.451	1.02 (0.64–1.62)	0.934
Group 4	1.72 (1.23–2.42)	0.002	1.76 (1.25–2.47)	0.001	1.32 (0.91–1.90)	0.146
P for trend		0.002		0.002		0.215
NGR						
Group 1	1.00 (Reference)		1.00 (Reference)		1.00 (Reference)	
Group 2	2.36 (1.36–4.08)	0.002	2.27 (1.31–3.94)	0.003	1.67 (0.95–2.93)	0.073
Group 3	2.58 (1.78–3.72)	< 0.001	2.40 (1.66–3.48)	< 0.001	1.82 (1.24–2.68)	0.002
Group 4	5.81 (3.87–8.73)	< 0.001	5.56 (3.70–8.36)	< 0.001	2.87 (1.79–4.61)	< 0.001
P for trend		< 0.001		< 0.001		< 0.001

Group 1: Low SHR and Low GV (SHR < 1.17 and GV < 23.40); Group 2: Low SHR and High GV (SHR < 1.17 and GV ≥ 23.40); Group 3: High SHR and Low GV (SHR ≥ 1.17 and GV < 23.40); Group 4: High SHR and High GV (SHR ≥ 1.17 and GV ≥ 23.40).

Variables	Model 1		Model2		Model3	
	HR (95%CI)	*P*	HR (95%CI)	*P*	HR (95%CI)	*P*
Pre-DM						
Group 1	1.00 (Reference)		1.00 (Reference)		1.00 (Reference)	
Group 2	2.54 (1.64–3.93)	< 0.001	2.42 (1.56–3.75)	< 0.001	2.15 (1.34–3.46)	0.001
Group 3	2.34 (1.51–3.65)	< 0.001	2.31 (1.49–3.60)	< 0.001	1.70 (1.07–2.72)	0.026
Group 4	2.16 (1.22–3.82)	0.008	2.18 (1.24–3.86)	0.007	1.50 (0.82–2.74)	0.192
P for trend		< 0.001		< 0.001		0.044
Model 1: unadjusted;						
Model 2: adjusted for age, gender and race						
Model 3 was further adjusted for APS - III, GCS, HR, RR, SpO2, Temperature, Cr, WBC, Platelet, AF, HF, Hypertension, MI, COPD, and Ventilation.						
Group 1: Low SHR and Low GV (SHR < 1.17 and GV < 23.40); Group 2: Low SHR and High GV (SHR < 1.17 and GV ≥ 23.40); Group 3: High SHR and Low GV (SHR ≥ 1.17 and GV < 23.40); Group 4: High SHR and High GV (SHR ≥ 1.17 and GV ≥ 23.40).						

Tests of the proportional hazards assumption showed that the hazard ratios for the combined SHR and GV groups remained constant over time in the NGR and PreDM subgroups (NGR: P = 0.509, Table S7; PreDM: P = 0.081, Table S9). In the DM subgroup, however, a nonconstant hazard ratio was observed (P = 0.015, Table S8), suggesting a time-dependent effect. Based on trends in Schoenfeld residuals (Fig. S1), day 2 after ICU admission was selected as the landmark time point. Landmark analysis showed no significant survival differences among the four SHR and GV groups within the first 2 days after ICU admission (P = 0.130). After 2 days, survival curves separated clearly (P = 0.008) (Fig. 5). Patients with both low SHR and low GV showed comparatively better 28-day survival, while those with elevated SHR and elevated GV experienced the poorest survival.

3.5. ROC curve analysis

The predictive performance of SHR, GV, and their combined metric for 28-day mortality is shown in Fig. 4A–C and Table S6. In the NGR group, the AUC of the combined SHR and GV metric was 0.686 (95% CI 0.642–0.731). This performance was superior to GV alone (AUC 0.626, P = 0.010) and showed a borderline advantage over SHR alone (AUC 0.670, P = 0.061). The discriminative ability of the combined metric was comparable to that of APS-III (AUC 0.689, P = 0.933).

In the PreDM group, the AUC of the combined metric was 0.628 (95% CI 0.581–0.676), which was higher than that of SHR alone (AUC 0.580, P = 0.004). No significant differences were observed when compared with GV alone (AUC 0.583, P = 0.096) or with SOFA and APS-III (AUCs of 0.615 and 0.616, respectively; both P > 0.05).

In the DM group, the AUC of the combined metric was 0.567 (95% CI 0.527–0.607). This value did not differ significantly from SHR alone (AUC 0.557, P = 0.158) or GV alone (AUC 0.544, P = 0.341). In contrast, APS-III (AUC 0.645, P = 0.001) and SOFA (AUC 0.618, P = 0.048) showed better predictive performance in this subgroup.

3.6 Sensitivity analysis

Several sensitivity analyses were conducted to test the stability of the main results. First, after removing patients who received glucose-lowering therapy, the findings from the Cox proportional hazards models remained largely consistent with the primary analysis(Table S10). Second, to limit the impact of outliers, we excluded patients with SHR or GV values below the 1st percentile or above the 99th percentile. After reanalysis, the association between the combined measure and all-cause mortality remained consistent with the main results (Table S11).

3.7. Feature selection

Variables included in the machine learning models for the NGR, PreDM, and DM subgroups were identified using the Boruta algorithm (Fig. 7). The results of Boruta analysis in the overall cohort are shown in Fig. S2. The top 15 variables ranked by importance were selected for subsequent model development and validation.

3.8 Development, evaluation, and explainability of the mortality risk prediction model

Figure 8 presents the ROC curves of different machine learning models in the testing set (Fig. 8A–C), with discriminative performance evaluated using the AUC. Overall, XGBoost and LGBM showed the best performance, followed by RF, whereas KNN and DT models performed less well. In the NGR subgroup (Fig. 8A), the AUCs were 0.786 for XGBoost, 0.782 for LGBM, 0.690 for RF, 0.646 for SVM, 0.585 for DT, and 0.547 for KNN. In the PreDM subgroup (Fig. 8B), the AUCs were 0.798 for LGBM, 0.794 for XGBoost, 0.719 for RF, 0.664 for DT, 0.584 for SVM, and 0.544 for KNN. In the DM subgroup (Fig. 8C), the AUCs were 0.851 for LGBM, 0.838 for XGBoost, 0.773 for RF, 0.717 for SVM, 0.677 for KNN, and 0.603 for DT.

Calibration curves are shown in Fig. 8G–I. Overall, the calibration curves for XGBoost and LGBM were closer to the reference line, suggesting better agreement between predicted risks and observed outcomes. Calibration error metrics also showed lower values for these two models, for example in the DM subgroup, the error was 0.080 for XGBoost and 0.085 for LGBM, whereas larger deviations were observed for SVM and KNN. DCA results are presented in Fig. 8D–F. Across a broad range of threshold probabilities, most models provided a higher net benefit than the treat-none approach, indicating

potential clinical value. Among them, XGBoost and LGBM showed more stable net benefit and superior performance across different subgroups.

Figure 9A–F displays SHAP scatter plots and mean importance bar plots for the best-performing models in each subgroup. The results indicate that both SHR and GV provided meaningful information for mortality prediction. In the PreDM subgroup, GV showed a more prominent contribution and jointly drove model predictions with key variables such as SAPS-II and GCS (Fig. 9B, E). In the NGR and DM subgroups, SHR retained a notable weight in the feature importance ranking, suggesting a relatively stable predictive value across different glucose metabolic states (Fig. 9A, C and Fig. 9D, F).

Figure S3 shows that all six machine learning models demonstrated acceptable discrimination for 28-day mortality in the overall cohort. LGBM (AUC = 0.796) and XGBoost (AUC = 0.776) achieved the best overall performance. Fig. S4 presents SHAP scatter plots and feature importance rankings for the overall prediction model. The results indicate that model predictions were mainly driven by key variables such as SAPS-II, vasoactive drug use, PT, and BUN. At the same time, SHR and GV were also ranked among the important features, indicating that both contributed valuable information to mortality risk prediction in the overall population (Fig. S4A, B).

4. Discussion

In this study, we examined the joint effects of SHR and GV on outcomes in critically ill patients with cerebrovascular disease. We placed particular emphasis on the modifying role of different glucose metabolic states. Our main findings show that elevations in SHR or GV are generally associated with worse clinical outcomes. Survival curves clearly demonstrated that patients with both high SHR and high GV had the lowest 28-day survival. After adjustment for multiple confounding factors, we observed marked population heterogeneity in these associations. In patients with NGR, both SHR and GV were independent risk factors, and their combined use substantially improved mortality risk prediction. In patients with PreDM, the combined metric also showed greater predictive potential than either indicator alone. These findings were further supported by machine learning analyses. Feature importance rankings confirmed that SHR and GV played key roles in the prediction models. Taken together, these findings indicate that combining acute and chronic glycemic markers yields a more precise method for risk stratification. This strategy may have practical implications for the clinical care of critically ill patients with cerebrovascular disease.

SHR reflects the magnitude of acute glucose dysregulation, measured by admission AG, relative to long-term glycemic status assessed by HbA1c. It therefore provides a more accurate representation of metabolic disturbance under acute stress. After a severe cerebrovascular event, the sympathetic nervous system and the hypothalamic–pituitary–adrenal axis activate quickly. Catecholamine and cortisol levels rise sharply. This response drives hepatic gluconeogenesis and glycogenolysis, and it worsens peripheral insulin resistance (27). As a result, blood glucose levels rise sharply over a short period, imposing an additional metabolic burden on neural tissue. Acute hyperglycemia can further

amplify energy metabolic impairment within the ischemic penumbra. It increases lactate accumulation and mitochondrial dysfunction and triggers pronounced oxidative stress responses (28). Experimental studies have shown that a hyperglycemic environment damages cerebral microvascular endothelium and tight junctions. This increases blood–brain barrier permeability and accelerates inflammatory infiltration and cerebral edema (29). These processes further disrupt blood–brain barrier integrity (30). In reperfusion models, hyperglycemia also promotes microthrombus formation and coagulation activation. This worsens perfusion disturbances and increases the risk of hemorrhagic transformation (31). Taken together, a higher SHR may function not only as an indicator of disease severity but also as a direct contributor to increased mortality risk in critically ill patients with cerebrovascular disease. This effect may act through several mechanisms, such as damage to the blood brain barrier, enhanced inflammatory responses, and disturbances in coagulation. In line with these mechanisms, multiple clinical studies have reported that elevated SHR is linked to higher short-term mortality and worse functional outcomes in ICU patients with ischemic stroke, as well as in broader acute ischemic stroke populations(32, 33). In cohorts with spontaneous intracerebral hemorrhage and thrombolysis-treated stroke, higher SHR has also been linked to hematoma expansion, symptomatic intracranial hemorrhage, and increased mortality. Systematic reviews and dose–response meta-analyses have further supported a positive link between SHR and the risk of unfavorable stroke outcomes (34–36).

Unlike the focus on acute admission-related glucose elevation, GV captures repeated rises and falls in glucose levels over a short period. Such fluctuations generate recurrent pulses of oxidative stress, overwhelm antioxidant defenses, and lead to sustained endothelial injury (37). In vitro studies have shown that alternating high and low glucose induces stronger inflammatory signaling and greater endothelial stress than persistent hyperglycemia. This finding suggests a higher susceptibility to microcirculatory imbalance (38). Animal studies further indicate that intermittent hyperglycemia enhances oxidative stress and activates nuclear factor–related pathways, thereby promoting apoptosis and tissue damage (39). At the central nervous system level, review studies have suggested that glucose fluctuations are linked to disrupted metabolic reprogramming of microglia and amplification of inflammatory responses. These processes may further aggravate ischemia–reperfusion injury and increase blood–brain barrier vulnerability (40). Clinical data suggest that, in patients with acute ischemic stroke, greater glucose variability measured by continuous glucose monitoring is frequently linked to worse neurological outcomes and a higher incidence of adverse events (17). In mechanical thrombectomy cohorts and related clinical studies, early systemic glucose fluctuations have also been associated with mortality risk. Glucose management strategies can influence the degree of variability, suggesting that GV provides complementary prognostic information beyond single glucose measurements (41, 42).

Taken together, our findings suggest that SHR mainly reflects an acute relative rise in glucose, whereas GV captures short-term glucose fluctuations. Assessing SHR and GV within a unified framework is therefore more likely to reflect the true spectrum of metabolic imbalance. Both associations remained independent after multivariable adjustment. After combined stratification, patients with both high SHR and high GV had the worst survival, and the risk gradient became clearer. ROC analyses further

supported the superiority of the combined metric over either indicator alone in patients with NGR and PreDM. This pattern may be explained by the concept of acute glucose toxicity. In individuals with long-term normoglycemia, a sudden relative increase in glucose more strongly reflects intense neuroendocrine stress. It is also more likely to trigger oxidative stress and endothelial injury, thereby amplifying metabolic burden in the ischemic penumbra and impairing microcirculation. As a result, the risk signal becomes more concentrated. Earlier stroke studies have likewise shown that the prognostic effect of stress hyperglycemia is stronger in patients without diabetes (43). After progression to PreDM, a key shift emerged in our results. Overall, the linear association between GV and mortality weakened, and risk became concentrated in two discordant patterns: low SHR with high GV and high SHR with low GV. This finding suggests that, in PreDM, a single abnormal dimension may already represent a high-risk pathway. Low SHR with high GV may reflect unstable glucose control with potential hypoglycemic fluctuations, whereas high SHR with low GV may reflect sustained stress hyperglycemia dominated by insulin resistance. Both pathways may contribute to increased infection risk and progression of organ dysfunction. In patients with diabetes, the combined metric did not form a stable risk gradient and showed clear time dependence. Landmark analysis indicated that early differences were modest and became apparent only over time. ROC analysis also showed that severity scores had stronger discriminative ability in this group. This may be related to an upward shift in baseline glucose levels due to chronic hyperglycemia. Because the denominator of SHR is influenced by HbA1c, part of the acute glucose rise may be masked. In addition, patients with diabetes more often receive exogenous insulin and intensive glucose-lowering therapy. Glucose variability in this setting may be driven more by treatment than by the underlying disease process. The concept of relative hypoglycemia and an upward shift in counterregulatory thresholds is also relevant, as it alters the physiological meaning of the same glucose level across populations (44). With respect to GV, meta-analyses and studies using continuous glucose monitoring in acute stroke have consistently reported that greater acute GV is linked to a higher risk of death (45). These findings provide external support for the signals observed in patients with NGR in our study. In subgroup analyses, the overall link between GV and 28-day mortality was modest. However, elevated GV was related to higher mortality in patients under 65 years, while this relationship was weaker in those aged 65 years or older. Previous ICU cohorts have also reported a weaker association between GV and mortality with increasing age. This suggests that higher baseline risk and blunted metabolic stress responses in older patients may dilute the relative harm of GV (46). Overall, our results highlight a central concept. The same glycemic abnormality may carry different physiological meanings and clinical pathways across glucose metabolic states. Therefore, combined assessment of SHR and GV is more appropriate for stratified analysis and individualized risk evaluation.

This study explored short-term outcomes in critically ill patients with cerebrovascular disease by focusing on heterogeneity in glycemic dysregulation. Unlike prior work that treated glycemic measures as uniform risk factors, we highlighted the central role of the metabolic background in risk interpretation. Our results show that the prognostic relevance of SHR and GV is not consistent across all populations. Assessing the two measures together allowed for clearer risk stratification in patients with NGR and in those with PreDM, but its value was markedly attenuated in patients with diabetes. This pattern suggests

that the same glycemic abnormality may reflect different physiological stress pathways under different metabolic states. We also integrated conventional regression models with interpretable machine learning methods. This approach supported the robustness of our findings and further clarified the relative contributions of SHR and GV across subgroups. By incorporating landmark analysis, we additionally observed that glycemia-related risk changed over the course of ICU hospitalization. This result provides a new viewpoint on the dynamic prognostic influence of glycemic dysregulation.

Several limitations warrant consideration. First, this study was retrospective and observational in nature. Although many covariates were adjusted for, residual confounding cannot be completely ruled out, and the results should not be interpreted as causal. Second, study inclusion depended on HbA1c and repeated glucose measurements. Some patients were therefore excluded, which may have affected the representativeness of the sample. Finally, the cohort came from a relatively homogeneous racial background and a single healthcare setting, which may restrict the generalizability of the findings to other regions and populations.

Conclusion

In critically ill patients with cerebrovascular disease, combining SHR and GV helps stratify 28-day mortality risk, and its performance varies by glucose metabolic status. The combined measure is stronger than either marker alone in NGR and PreDM.

Abbreviations

ABG Admission blood glucose, AF Atrial fibrillation, AG Average glucose, AMI Acute myocardial infarction, APS-III Acute Physiology Score III, AUC Area under the curve, BUN Blood urea nitrogen, CI Confidence interval, CITI Collaborative Institutional Training Initiative, COPD Chronic obstructive pulmonary disease, Cr Creatinine, CV Coefficient of variation, DCA Decision curve analysis, DM Diabetes mellitus, DT Decision tree, GCS Glasgow Coma Scale, GV Glycemic variability, Hb Hemoglobin, HbA1c Glycated hemoglobin, HF Heart failure, HR Heart rate, ICD-9 International Classification of Diseases, Ninth Revision, ICD-10 International Classification of Diseases, Tenth Revision, ICU Intensive care unit, IQR Interquartile range, KM Kaplan–Meier, KNN k-nearest neighbors, LGBM Light gradient boosting machine, MI Myocardial infarction, MIMIC-IV Medical Information Mart for Intensive Care IV, NBPM Mean noninvasive blood pressure, NGR Normal glucose regulation, PreDM Prediabetes mellitus, PT Prothrombin time, RBC Red blood cell count, RCS Restricted cubic splines, RF Random forest, ROC Receiver operating characteristic, RR Respiratory rate, SAPS-II Simplified Acute Physiology Score II, SD Standard deviation, SHAP Shapley additive explanations, SHR Stress hyperglycemia ratio, SOFA Sequential Organ Failure Assessment, SQL Structured Query Language, SVM Support vector machine, T2DM Type 2 diabetes mellitus, VIF Variance inflation factor, WBC White blood cell count, XGBoost Extreme gradient boosting.

Declarations

Ethics approval and consent to participate

This study was conducted in accordance with the Declaration of Helsinki. The MIMIC-IV database was approved by the Institutional Review Boards (IRBs) of Beth Israel Deaconess Medical Center and the Massachusetts Institute of Technology. The requirement for written informed consent was waived because the database contains de-identified patient information and the study did not affect clinical care.

Consent for publication

Not applicable.

Availability of data and materials

This study analyzed publicly available datasets, which can be accessed here: https://physionet.org/content/

Competing interests

The authors declare that the research was conducted in the absence of any commercial or financial relationships that could be construed as a potential conflict of interest.

Funding

The author(s) declare that financial support was received for the research and/or publication of this article. This work was supported by the **National Natural Science Foundation of China (Grant No. 8257145391)**.

Authors' contributions

Zhantao Cao: Conceptualization, Data curation, Formal Analysis, Funding acquisition, Investigation, Methodology, Project administration, Resources, Software, Supervision, Validation, Visualization, Writing–original draft, Writing–review & editing.

Siyu Liu: Data curation, Investigation, Software, Writing–review & editing.

Yue Wei: Data curation, Investigation, Software, Writing–review & editing.

Dongxin Liu: Investigation, Supervision, Writing–review & editing.

Yao Li: Formal Analysis, Project administration, Writing–review & editing.

Guoju Dong: Software, Funding acquisition, Writing–review & editing.

All authors have read and approved the final manuscript.

Acknowledgements

Not applicable.

References

1. Global. regional, and national burden of stroke and its risk factors, 1990–2021: a systematic analysis for the Global Burden of Disease Study 2021. Lancet Neurol. 2024;23:973–1003. 10.1016/s1474-4422(24)00369-7.
2. Li XY, Kong XM, Yang CH et al. Global, regional, and national burden of ischemic stroke, 1990–2021: an analysis of data from the global burden of disease study 2021. EClinicalMedicine. (2024) 75:102758. 10.1016/j.eclinm.2024.102758
3. Kanda M, Sato T, Yoshida Y, Kuwabara H, Kobayashi Y, Inoue T. Effect of admission in the stroke care unit versus intensive care unit on in-hospital mortality in patients with acute ischemic stroke. BMC Neurol. 2023;23:402. 10.1186/s12883-023-03454-6.
4. Wu D, Shen S, Luo D. Association of lactate-to-albumin ratio with in-hospital and intensive care unit mortality in patients with intracerebral hemorrhage. Front Neurol. 2023;14:1198741. 10.3389/fneur.2023.1198741.
5. Huang ZG, Gao JW, Chen ZT, et al. Comprehensive Multiple Risk Factor Control in Type 2 Diabetes to Mitigate Heart Failure Risk: Insights From a Prospective Cohort Study. Diabetes Care. 2024;47:1818–25. 10.2337/dc24-0864.
6. Schlesinger S, Neuenschwander M, Barbaresko J, et al. Prediabetes and risk of mortality, diabetes-related complications and comorbidities: umbrella review of meta-analyses of prospective studies. Diabetologia. 2022;65:275–85. 10.1007/s00125-021-05592-3.
7. Jiang Z, Wang K, Duan H, et al. Association between stress hyperglycemia ratio and prognosis in acute ischemic stroke: a systematic review and meta-analysis. BMC Neurol. 2024;24:13. 10.1186/s12883-023-03519-6.
8. Fadini GP. Perturbation of Glucose Homeostasis During Acute Illness: Stress Hyperglycemia and Relative Hypoglycemia. Diabetes Care. 2022;45:769–71. 10.2337/dci21-0069.
9. Yao M, Hao Y, Wang T, et al. A review of stress-induced hyperglycaemia in the context of acute ischaemic stroke: Definition, underlying mechanisms, and the status of insulin therapy. Front Neurol. 2023;14:1149671. 10.3389/fneur.2023.1149671.
10. Chen Q, Su H, Yu X, et al. The stress hyperglycemia ratio improves the predictive ability of the GRACE score for in-hospital mortality in patients with acute myocardial infarction. Hellenic J Cardiol. 2023;70:36–45. 10.1016/j.hjc.2022.12.012.
11. Pan L, Li Z, Li C, et al. Stress hyperglycemia ratio and neutrophil to lymphocyte ratio are reliable predictors of new-onset atrial fibrillation in patients with acute myocardial infarction. Front Cardiovasc Med. 2022;9:1051078. 10.3389/fcvm.2022.1051078.

12. Martinez M, Santamarina J, Pavesi A, Musso C, Umpierrez GE. Glycemic variability and cardiovascular disease in patients with type 2 diabetes. BMJ Open Diabetes Res Care. 2021;9. 10.1136/bmjdrc-2020-002032.
13. Belli M, Bellia A, Sergi D, Barone L, Lauro D, Barillà F. Glucose variability: a new risk factor for cardiovascular disease. Acta Diabetol. 2023;60:1291–9. 10.1007/s00592-023-02097-w.
14. Lu Z, Tao G, Sun X, et al. Association of Blood Glucose Level and Glycemic Variability With Mortality in Sepsis Patients During ICU Hospitalization. Front Public Health. 2022;10:857368. 10.3389/fpubh.2022.857368.
15. Li AQ, Zhang F. Blood glucose variability impacts heart rate dynamics in older type 2 diabetic and coronary heart disease patients. World J Diabetes. 2025;16:110722. 10.4239/wjd.v16.i10.110722.
16. Liang S, Tian X, Gao F, et al. Prognostic significance of the stress hyperglycemia ratio and admission blood glucose in diabetic and nondiabetic patients with spontaneous intracerebral hemorrhage. Diabetol Metab Syndr. 2024;16:58. 10.1186/s13098-024-01293-0.
17. Palaiodimou L, Lioutas VA, Lambadiari V, et al. Glycemic variability of acute stroke patients and clinical outcomes: a continuous glucose monitoring study. Ther Adv Neurol Disord. 2021;14:17562864211045876. 10.1177/17562864211045876.
18. Johnson AEW, Bulgarelli L, Shen L, et al. MIMIC-IV, a freely accessible electronic health record dataset. Sci Data. 2023;10:1. 10.1038/s41597-022-01899-x.
19. Zhang T, Zhang M, Fan H, et al. Thiamine use and short-term prognosis in critical cerebrovascular disease: a propensity score matched retrospective analysis from the MIMIC-IV database. BMC Neurol. 2025;25:450. 10.1186/s12883-025-04478-w.
20. Li Y, Yu L, Fu M, et al. Prognostic value of glucose-to-lymphocyte ratio for all-cause mortality and consciousness impairment in critically ill cerebrovascular disease patients. Eur J Med Res. 2025;30:1189. 10.1186/s40001-025-03378-6.
21. Nathan DM, Kuenen J, Borg R, Zheng H, Schoenfeld D, Heine RJ. Translating the A1C assay into estimated average glucose values. Diabetes Care. 2008;31:1473–8. 10.2337/dc08-0545.
22. Wang F, Guo Y, Tang Y, et al. Combined assessment of stress hyperglycemia ratio and glycemic variability to predict all-cause mortality in critically ill patients with atherosclerotic cardiovascular diseases across different glucose metabolic states: an observational cohort study with machine learning. Cardiovasc Diabetol. 2025;24:199. 10.1186/s12933-025-02762-0.
23. Wang F, Guo Y, Jiao C, et al. Simultaneous Assessment of Stress Hyperglycemia Ratio and Glucose Variability to Predict All-cause Mortality in Sepsis Patients Across Different Glucose Metabolic States: an Observational Cohort Study With Interpretable Machine Learning Approach. Int J Surg. 2025. 10.1097/JS9.0000000000003525.
24. Yu Q, Fu Q, Ma X et al. Impact of glycemic control metrics on short- and long-term mortality in transcatheter aortic valve replacement patients: a retrospective cohort study from the MIMIC-IV database. Cardiovasc Diabetol. (2025) 24:135. 10.1186/s12933-025-02684-x

25. Diagnosis and classification of diabetes mellitus. Diabetes Care. 2014;37(Suppl 1):S81–90. 10.2337/dc14-S081.
26. Yan F, Chen X, Quan X, Wang L, Wei X, Zhu J. Association between the stress hyperglycemia ratio and 28-day all-cause mortality in critically ill patients with sepsis: a retrospective cohort study and predictive model establishment based on machine learning. Cardiovasc Diabetol. 2024;23:163. 10.1186/s12933-024-02265-4.
27. Song G, Liu X, Lu Z, et al. Relationship between stress hyperglycaemic ratio (SHR) and critical illness: a systematic review. Cardiovasc Diabetol. 2025;24:188. 10.1186/s12933-025-02751-3.
28. Alabdali MM, Alrasheed AS, Alghirash FA, et al. Stress Hyperglycemia as a Prognostic Indicator of the Clinical Outcomes in Patients with Stroke: A Comprehensive Literature Review. Biomedicines. 2025;13. 10.3390/biomedicines13081834.
29. Guo Y, Dong L, Gong A, et al. Damage to the blood–brain barrier and activation of neuroinflammation by focal cerebral ischemia under hyperglycemic condition. Int J Mol Med. 2021;48. 10.3892/ijmm.2021.4975.
30. Wu Q, Wei C, Guo S, et al. Acute iron overload aggravates blood-brain barrier disruption and hemorrhagic transformation after transient focal ischemia in rats with hyperglycemia. IBRO Neurosci Rep. 2022;13:87–95. 10.1016/j.ibneur.2022.06.006.
31. Leng C, Lin K, Zhou M, et al. Apolipoprotein E deficiency exacerbates blood-brain barrier disruption and hyperglycemia-associated hemorrhagic transformation after ischemic stroke. J Stroke Cerebrovasc Dis. 2024;33:107987. 10.1016/j.jstrokecerebrovasdis.2024.107987.
32. Pan H, Xiong Y, Huang Y, Zhao J, Wan H. Association between stress hyperglycemia ratio with short-term and long-term mortality in critically ill patients with ischemic stroke. Acta Diabetol. 2024;61:859–68. 10.1007/s00592-024-02259-4.
33. Xiao S, Gao M, Hu S, Cao S, Teng L, Xie X. Association between stress hyperglycemia ratio and functional outcomes in patients with acute ischemic stroke. BMC Neurol. 2024;24:288. 10.1186/s12883-024-03795-w.
34. Chu H, Huang C, Tang Y, Dong Q, Guo Q. The stress hyperglycemia ratio predicts early hematoma expansion and poor outcomes in patients with spontaneous intracerebral hemorrhage. Ther Adv Neurol Disord. 2022;15:17562864211070681. 10.1177/17562864211070681.
35. Krongsut S, Kaewkrasaesin C. Performance comparison of stress hyperglycemia ratio for predicting fatal outcomes in patients with thrombolyzed acute ischemic stroke. PLoS ONE. 2024;19:e0297809. 10.1371/journal.pone.0297809.
36. Huang YW, Yin XS, Li ZP. Association of the stress hyperglycemia ratio and clinical outcomes in patients with stroke: A systematic review and meta-analysis. Front Neurol. 2022;13:999536. 10.3389/fneur.2022.999536.
37. Offler LJ, Wells LK, Palmer TM. The Impact of Glycaemic Variability on Vascular Dysfunction in Diabetes. Biomolecules. 2025;15. 10.3390/biom15111544.

38. Toma L, Sanda GM, Stancu CS, Niculescu LS, Raileanu M, Sima AV. Oscillating Glucose Induces the Increase in Inflammatory Stress through Ninjurin-1 Up-Regulation and Stimulation of Transport Proteins in Human Endothelial Cells. Biomolecules. 2023;13. 10.3390/biom13040626.
39. Zhang W, Zhao S, Li Y, Peng G, Han P. Acute blood glucose fluctuation induces myocardial apoptosis through oxidative stress and nuclear factor-κB activation. Cardiology. 2013;124:11–7. 10.1159/000345436.
40. Watt C, Sanchez-Rangel E, Hwang JJ. Glycemic Variability and CNS Inflammation: Reviewing the Connection. Nutrients. (2020) 12. 10.3390/nu12123906
41. Deng J, Li L, Cao F, et al. Systemic Glycemic Variation Predicts Mortality of Acute Ischemic Stroke After Mechanical Thrombectomy: A Prospective Study Using Continuous Glucose Monitoring. Front Neurol. 2022;13:817033. 10.3389/fneur.2022.817033.
42. Gutiérrez-Zúñiga R, Alonso de Leciñana M, Delgado-Mederos R et al. Beyond hyperglycemia: glycaemic variability as a prognostic factor after acute ischemic stroke. Neurologia (Engl Ed). (2023) 38:150–8. 10.1016/j.nrleng.2020.06.017
43. Muscari A, Falcone R, Recinella G, et al. Prognostic significance of diabetes and stress hyperglycemia in acute stroke patients. Diabetol Metab Syndr. 2022;14:126. 10.1186/s13098-022-00896-9.
44. Schwartz MW, Krinsley JS, Faber CL, Hirsch IB, Brownlee M. Brain Glucose Sensing and the Problem of Relative Hypoglycemia. Diabetes Care. 2023;46:237–44. 10.2337/dc22-1445.
45. Lin J, Cai C, Xie Y, Yi L. Acute glycemic variability and mortality of patients with acute stroke: a meta-analysis. Diabetol Metab Syndr. 2022;14:69. 10.1186/s13098-022-00826-9.
46. Lu L, Lu Y, Gao C, Zhang N. Age moderates the relationships between obesity, glucose variability, and intensive care unit mortality: a retrospective cohort study. J Intensive Care. 2021;9:68. 10.1186/s40560-021-00582-4.

Figures

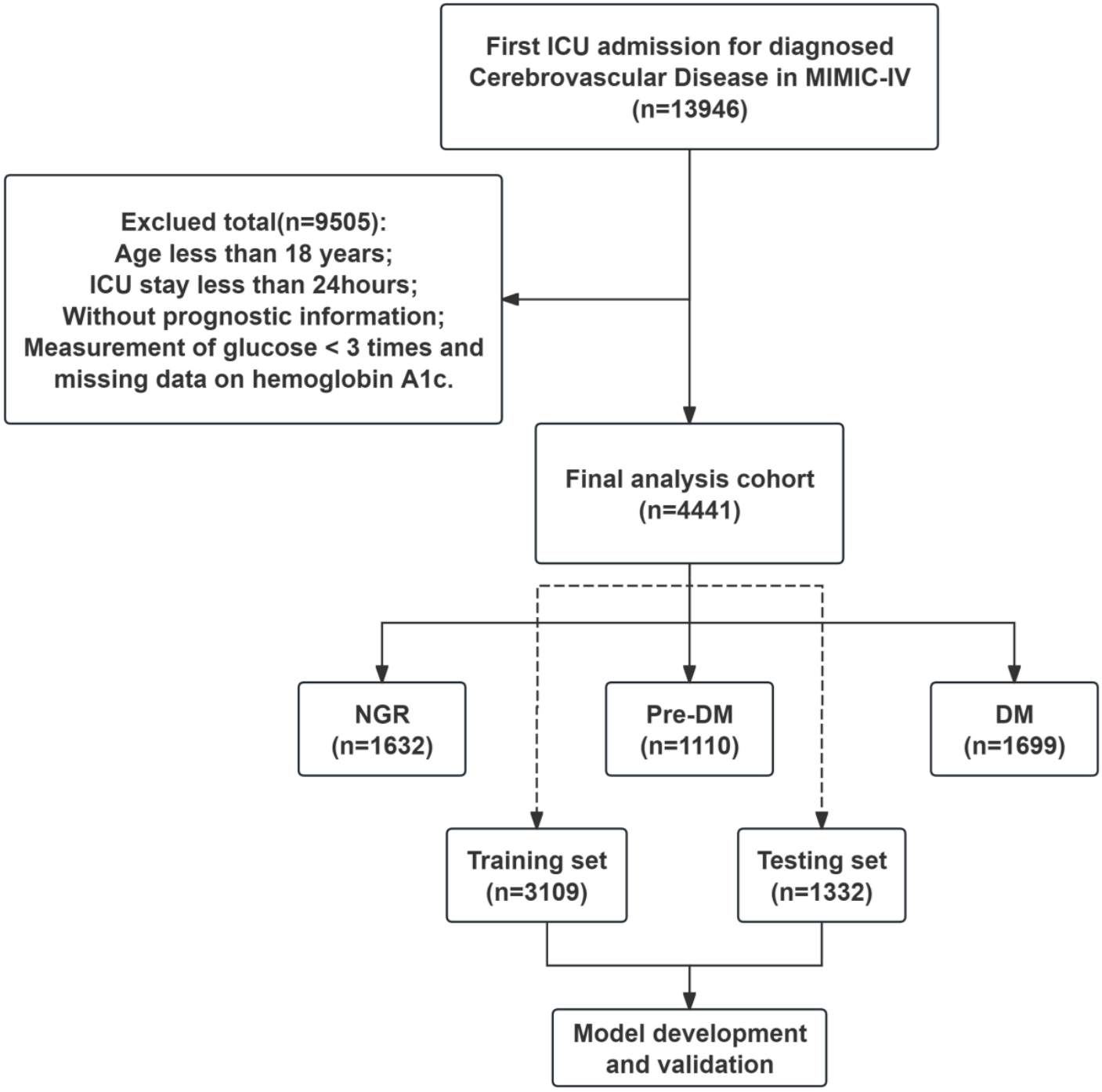


Figure 1

Study flowchart of cohort selection from MIMIC-IV.

Legend: Flow diagram showing inclusion and exclusion of adult ICU patients with cerebrovascular disease from the MIMIC-IV database. Patients were restricted to the first ICU stay, ICU length of stay ≥24 h, available outcome and key covariates, ≥3 glucose measurements during ICU monitoring, and available HbA1c for calculation of stress hyperglycemia ratio (SHR). The final analytic cohort was stratified by

glucose metabolic status into normal glucose regulation (NGR), prediabetes (PreDM), and diabetes mellitus (DM).

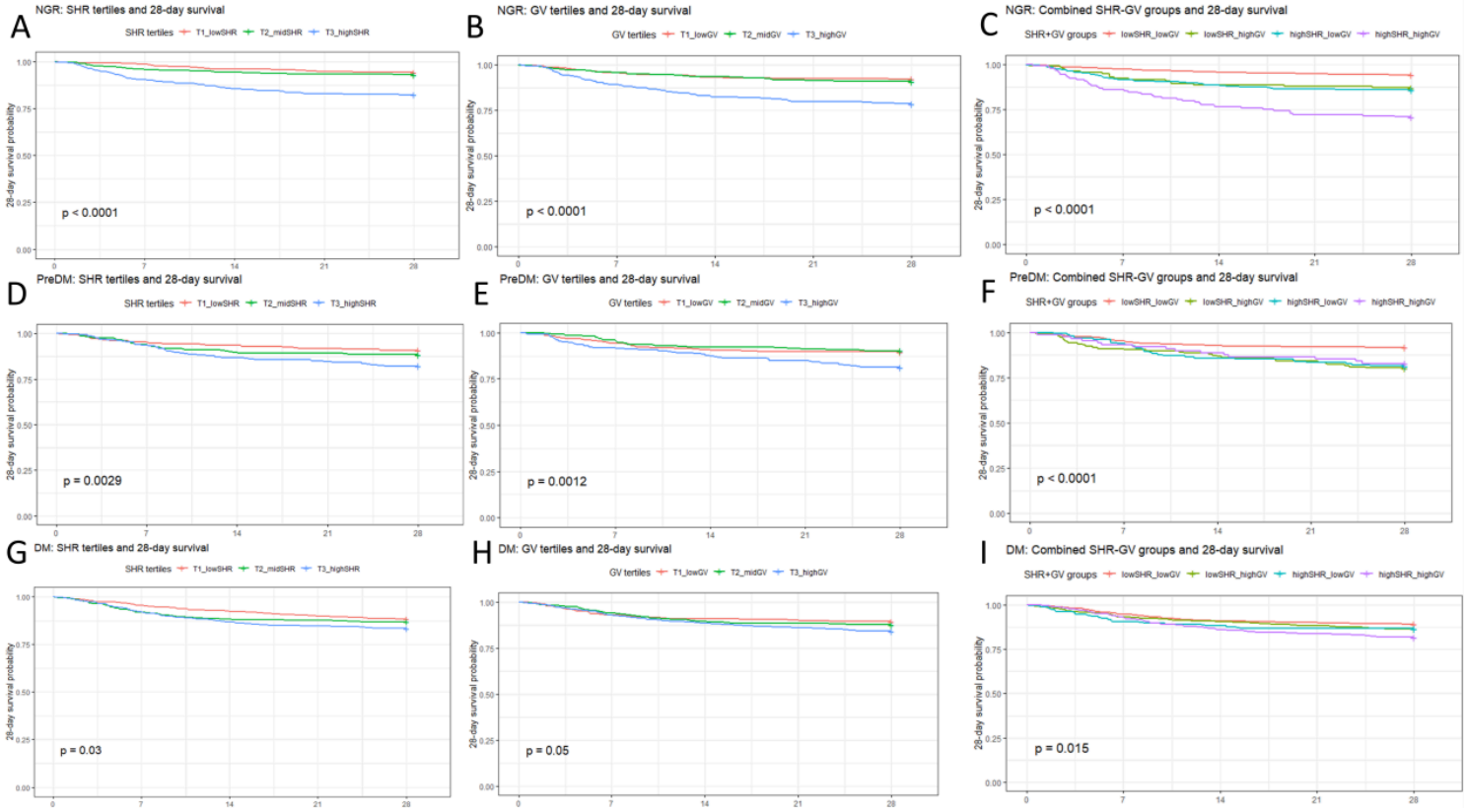


Figure 2

Kaplan–Meier survival by SHR, GV, and combined SHR–GV groups.

Legend: Kaplan–Meier curves for 28-day survival stratified by glucose metabolic status. (A–C) NGR; (D–F) PreDM; (G–I) DM. Panels show survival by SHR tertiles (A, D, G), GV tertiles (B, E, H), and combined SHR–GV categories (C, F, I). SHR and GV were categorized into tertiles; for the combined analysis, “high” denotes the highest tertile and “low” denotes the lower two tertiles, forming four groups: low SHR+low GV, low SHR+high GV, high SHR+low GV, and high SHR+high GV. P values shown in each panel are from log-rank tests.

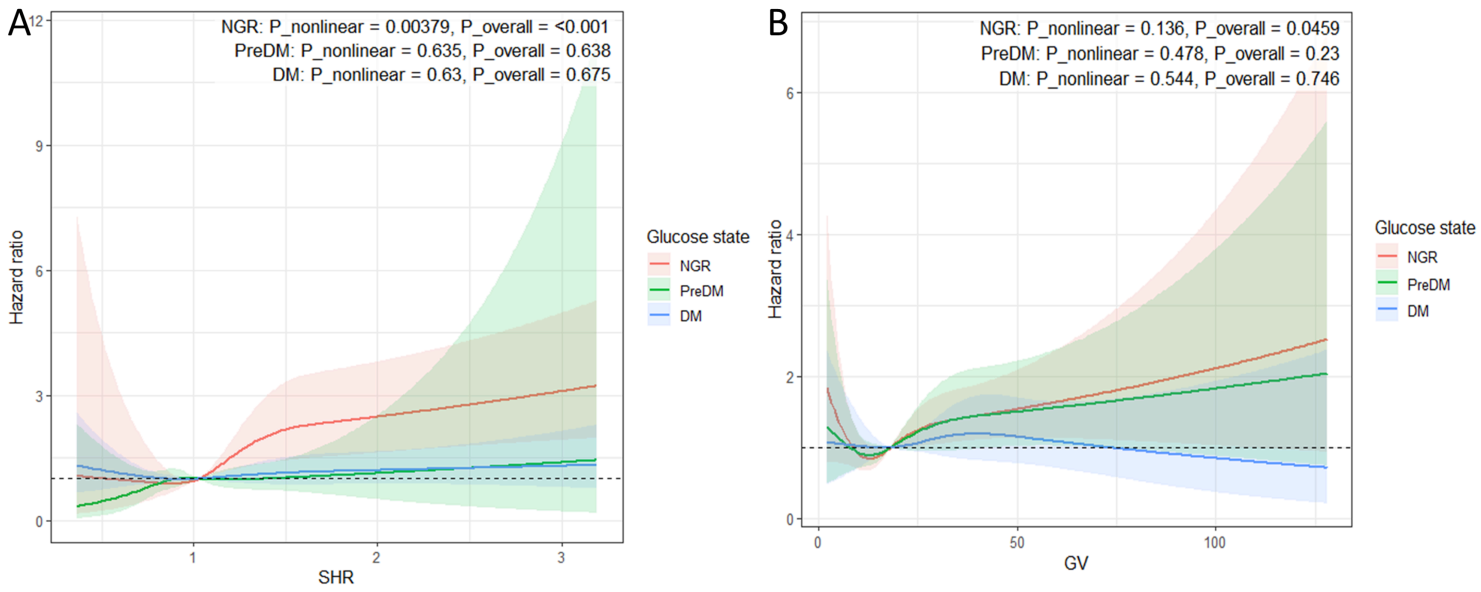


Figure 3

Restricted cubic spline associations of SHR and GV with 28-day mortality.

Legend: Restricted cubic spline curves showing the dose–response association between (A) SHR and (B) GV with hazard ratios (HRs) for 28-day all-cause mortality, stratified by glucose metabolic status (NGR, PreDM, DM). Solid lines indicate adjusted HRs and shaded bands represent 95% confidence intervals; the horizontal dashed line denotes HR=1. P values for overall and nonlinear associations are displayed within each panel. Models were adjusted as described in the fully adjusted Cox model in the Methods.

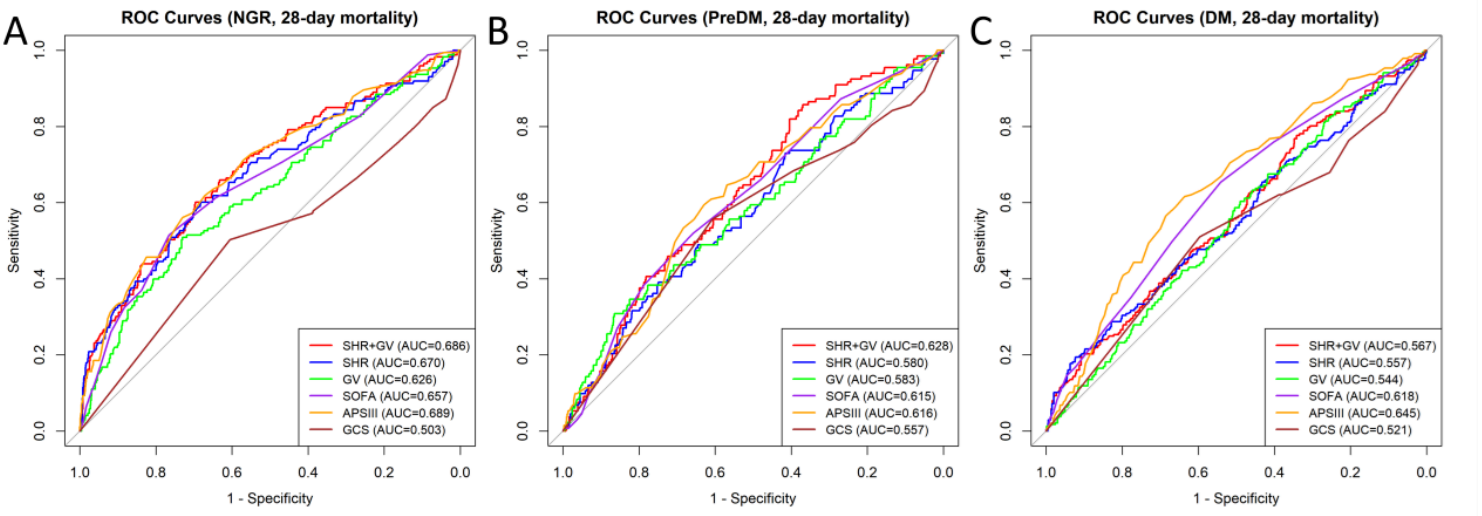


Figure 4

ROC curves comparing SHR, GV, combined metric, and severity scores.

Legend: Receiver operating characteristic (ROC) curves for predicting 28-day mortality in (A) NGR, (B) PreDM, and (C) DM. Curves compare SHR alone, GV alone, the combined SHR+GV metric, and commonly used severity/neurologic scores (e.g., SOFA, APS-III, and GCS). Areas under the curve (AUCs) are shown in each panel legend.

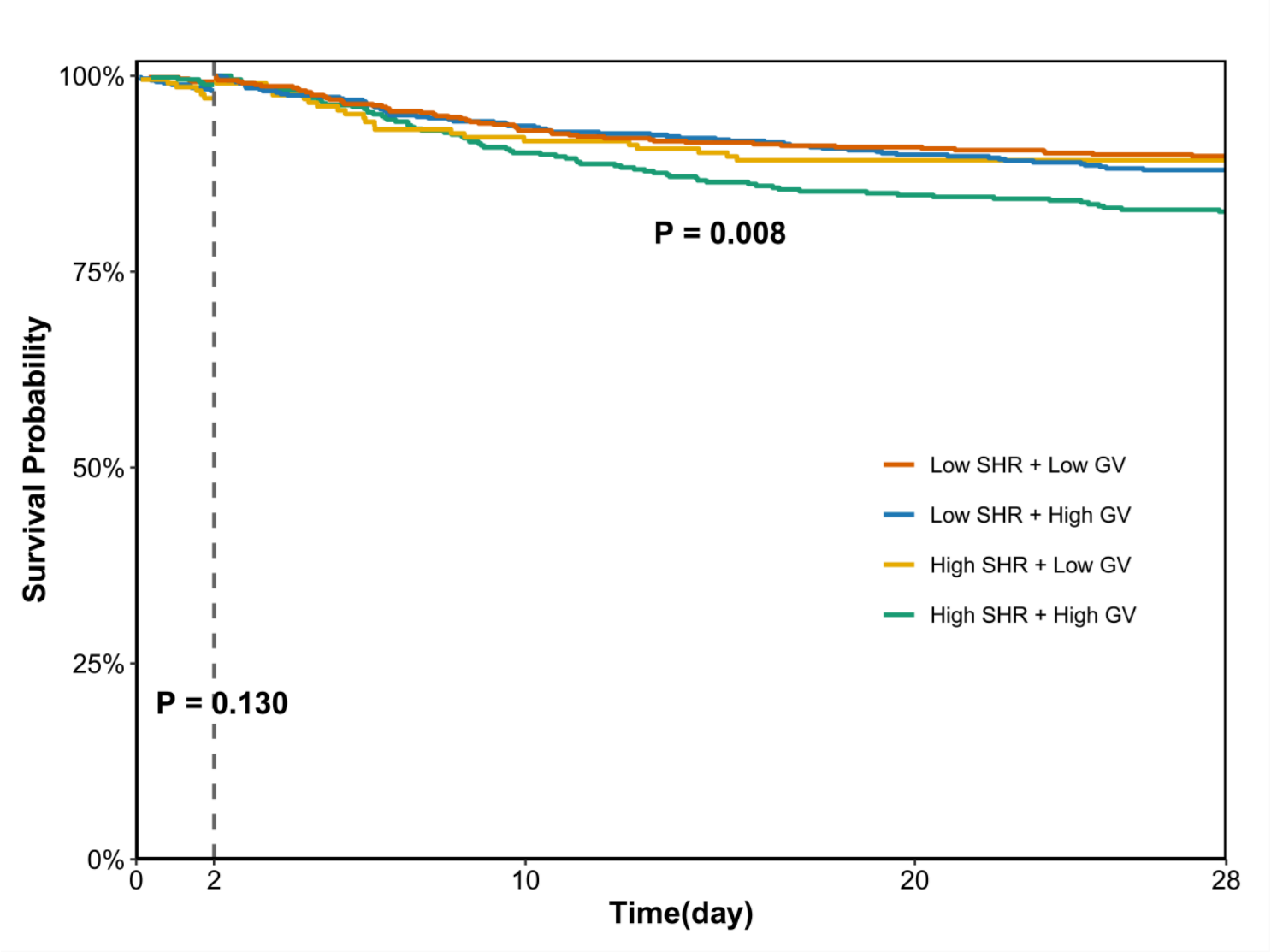


Figure 5

Landmark analysis of combined SHR–GV groups for 28-day.

Legend: Landmark Kaplan–Meier analysis evaluating time-varying separation among combined SHR–GV groups. A vertical dashed line marks the landmark time point at day 2 after ICU admission. P values indicate between-group differences within the first 2 days and after day 2, respectively. Curves correspond to four combined categories: low SHR+low GV, low SHR+high GV, high SHR+low GV, and high SHR+high GV.

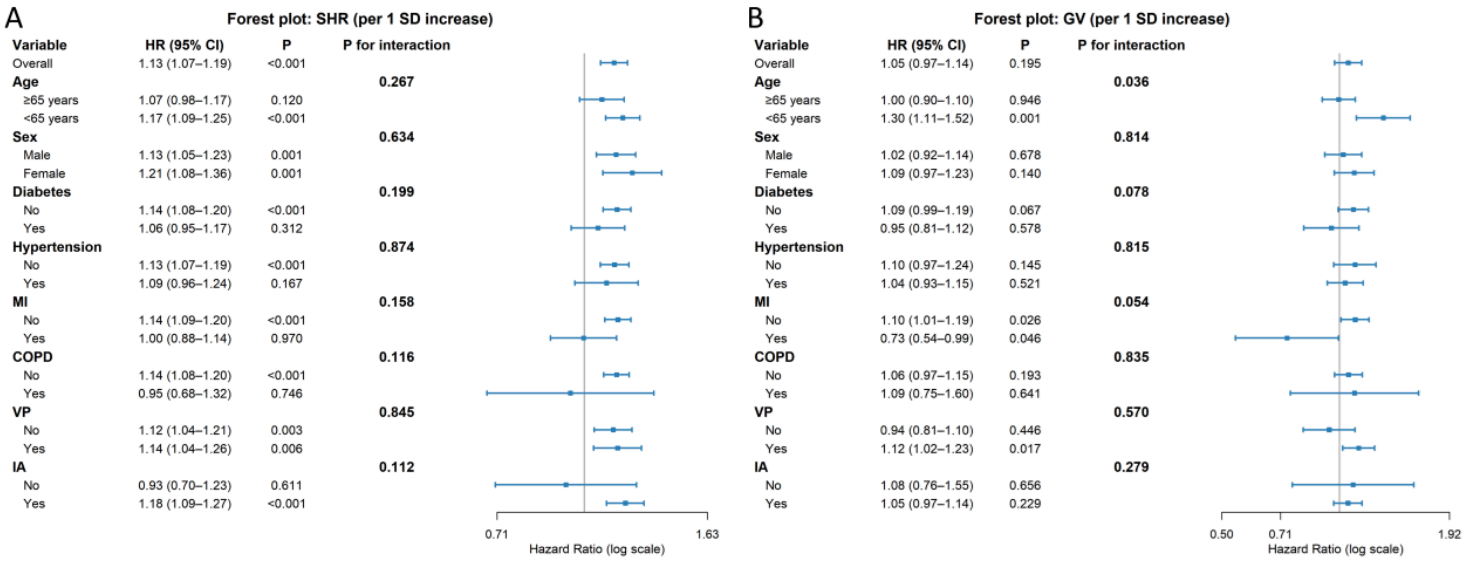


Figure 6

Subgroup analyses for SHR and GV.

Legend: Forest plots showing adjusted hazard ratios (HRs) and 95% confidence intervals for 28-day mortality per 1 standard deviation (SD) increase in (A) SHR and (B) GV across prespecified subgroups (e.g., age, sex, diabetes, hypertension, myocardial infarction, COPD, vasoactive drug use, and other clinical strata). P values for within-subgroup associations and interaction tests are shown. HRs are plotted on a log scale; the vertical reference line indicates HR=1.

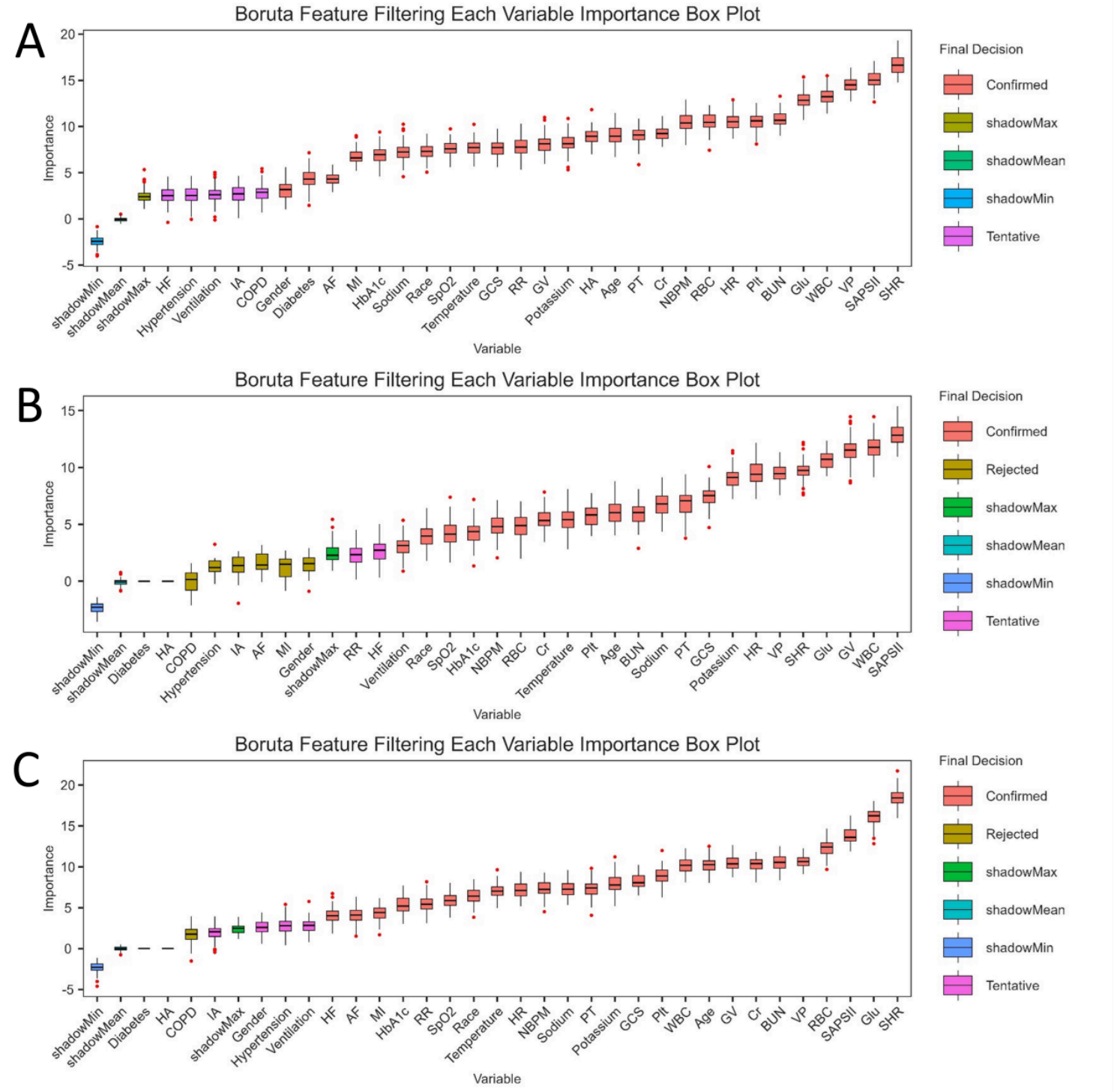


Figure 7

Boruta feature selection results by glucose metabolic status.

Legend: Boruta feature selection boxplots showing variable importance for mortality prediction in (A) NGR, (B) PreDM, and (C) DM. Colored boxes indicate Boruta decisions (confirmed, tentative, rejected) relative to shadow features (shadowMax/Mean/Min). Variables are ordered by importance, and the confirmed features informed subsequent model development (top-ranked variables selected as described in Methods).

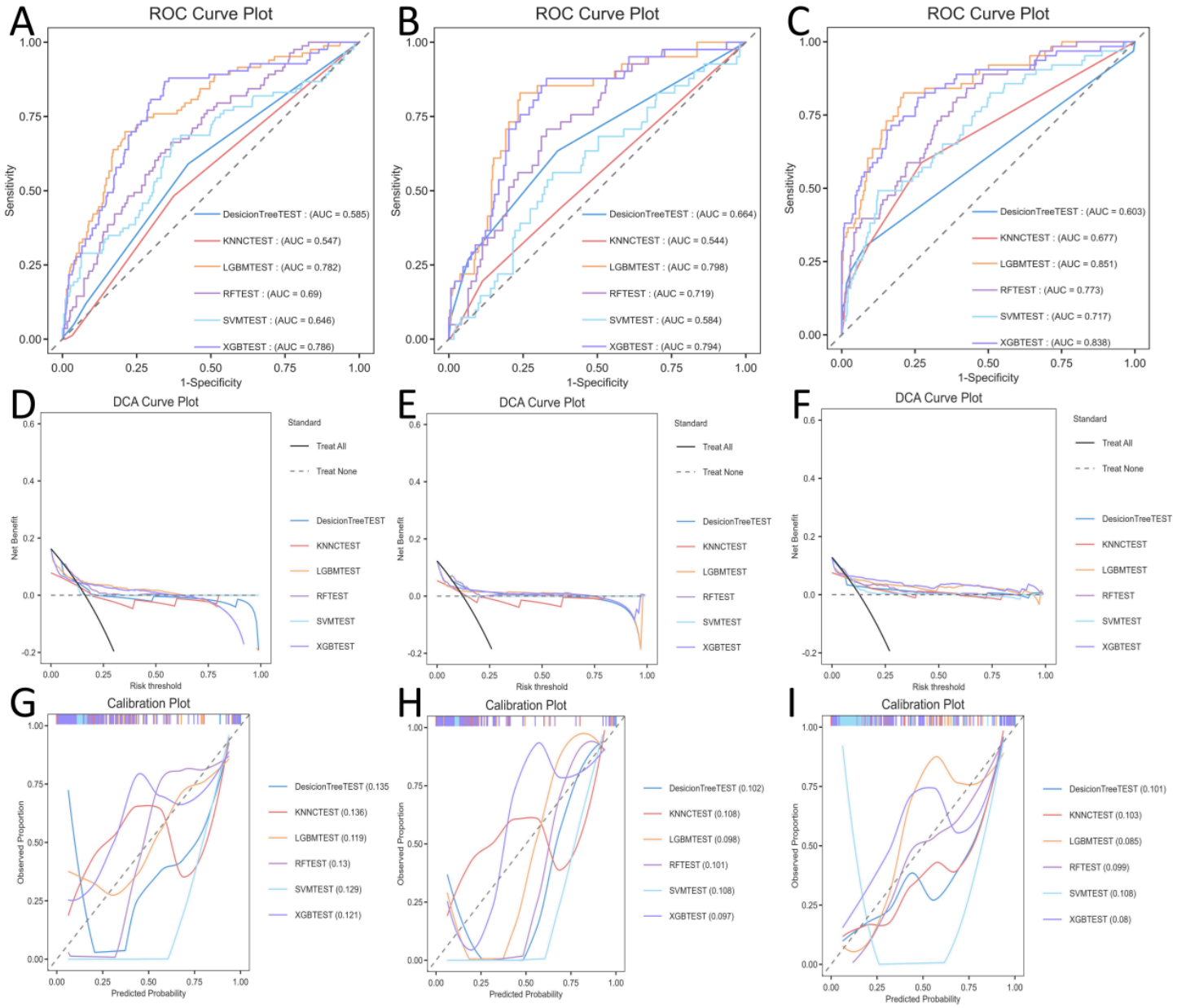


Figure 8

Machine learning model performance: ROC, decision curves, and calibration.

Legend: Performance of six machine learning models for 28-day mortality prediction in the testing set across glucose metabolic strata. (A–C) ROC curves in NGR, PreDM, and DM comparing random forest (RF), k-nearest neighbors (KNN), decision tree (DT), support vector machine (SVM), extreme gradient boosting (XGBoost), and light gradient boosting machine (LGBM), with AUCs indicated. (D–F) Decision curve analysis (DCA) showing net benefit across threshold probabilities, including treat-all and treat-none references. (G–I) Calibration plots comparing predicted and observed risks, with the diagonal line indicating perfect calibration.

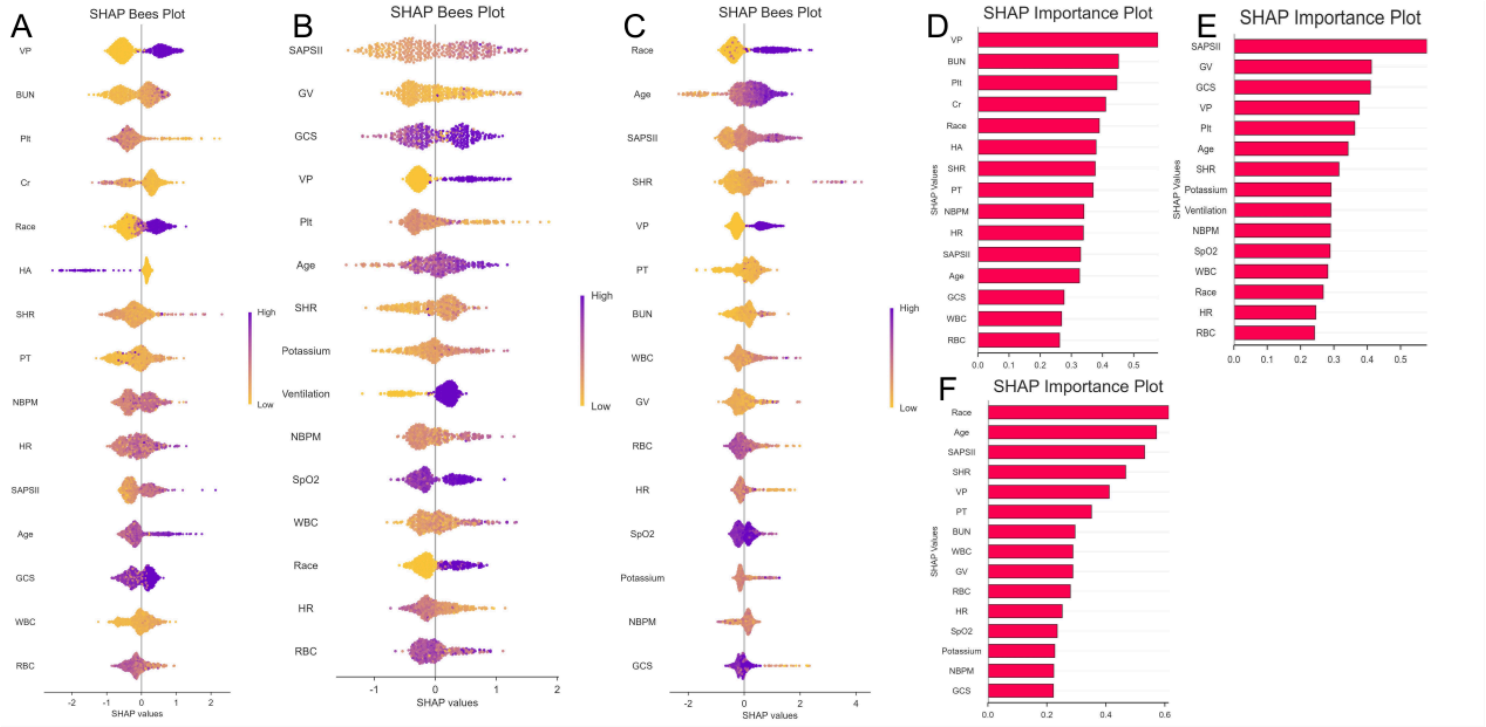


Figure 9

SHAP explainability for the best-performing models in each subgroup.

Legend: Shapley additive explanations (SHAP) for the best-performing model within each glucose metabolic subgroup. (A–C) SHAP beeswarm plots displaying the distribution of feature effects on predicted 28-day mortality risk; color reflects feature value (low to high). (D–F) Mean absolute SHAP value bar plots ranking global feature importance. Key predictors include severity indicators and metabolic measures, with SHR and/or GV contributing meaningfully depending on subgroup.

Supplementary Files

This is a list of supplementary files associated with this preprint. Click to download.

- Supplementarymaterials.docx
- Graphicalabstract.tif